Developmental Biology 368 (2012) 312–322

Contents lists available at SciVerse ScienceDirect

Developmental Biology

journal homepage: www.elsevier.com/locate/developmentalbiology

Multiple roles for the Na,K-ATPase subunits, Atp1a1 and Fxyd1, during brain ventricle development

Jessica T. Chang [a,b], Laura Anne Lowery [a,b,1], Hazel Sive [a,b,*]

[a] Whitehead Institute for Biomedical Research, Nine Cambridge Center, Cambridge, MA 02142, United States
[b] Massachusetts Institute of Technology, Department of Biology, 31 Ames Street, Cambridge, MA 02139, United States

ARTICLE INFO

Article history:
Received 17 December 2011
Received in revised form
29 May 2012
Accepted 29 May 2012
Available online 7 June 2012

Keywords:
Brain ventricles
Na,K-ATPase
Fxyd1
Atp1a1
Neuroepithelium
Permeability

ABSTRACT

Formation of the vertebrate brain ventricles requires both production of cerebrospinal fluid (CSF), and its retention in the ventricles. The Na,K-ATPase is required for brain ventricle development, and we show here that this protein complex impacts three associated processes. The first requires both the alpha subunit (Atp1a1) and the regulatory subunit, Fxyd1, and leads to formation of a cohesive neuroepithelium, with continuous apical junctions. The second process leads to modulation of neuroepithelial permeability, and requires Atp1a1, which increases permeability with partial loss of function and decreases it with overexpression. In contrast, *fxyd1* overexpression does not alter neuroepithelial permeability, suggesting that its activity is limited to neuroepithelium formation. RhoA regulates both neuroepithelium formation and permeability, downstream of the Na,K-ATPase. A third process, likely to be CSF production, is RhoA-independent, requiring Atp1a1, but not Fxyd1. Consistent with a role for Na,K-ATPase pump function, the inhibitor ouabain prevents neuroepithelium formation, while intracellular Na^+ increases after Atp1a1 and Fxyd1 loss of function. These data include the first reported role for Fxyd1 in the developing brain, and indicate that the Na,K-ATPase regulates three aspects of brain ventricle development essential for normal function: formation of a cohesive neuroepithelium, restriction of neuroepithelial permeability, and production of CSF.

Introduction

The vertebrate brain ventricular system comprises an essential set of interconnected cavities, filled with cerebrospinal fluid (CSF). Initially, CSF is produced by the neuroepithelium lining the ventricles (Welss, 1934), and later also by the choroid plexus, a series of vascularized secretory organs (Brown et al., 2004; Speake et al., 2001). Brain ventricle development requires a cohesive neuroepithelium with apical and basal polarity that can retain fluid, a correctly shaped epithelium, production of CSF, and expansion of the epithelium to accommodate the CSF (Ciruna et al., 2006; Gutzman and Sive, 2010; Hong and Brewster, 2006; Lowery and Sive, 2005, 2009; Zhang et al., 2010). We previously demonstrated a requirement for the Na,K-ATPase during zebrafish brain ventricle development. Specifically, the *snakehead* (*snk* ^{to273a}) mutant, corresponding to a point mutation in the alpha subunit (*atp1a1*) of the Na,K-ATPase, fails to inflate its brain ventricles (Lowery and Sive, 2005). This led to the hypothesis that *snk* ^{to273a} ventricles fail to inflate because CSF is not produced (Lowery and Sive, 2005; Zhang et al., 2010).

The Na,K-ATPase is a protein complex composed of an alpha, beta, and FXYD subunit. Alpha and beta subunits form a heterodimer that is the minimal functional unit for catalytic activity and ion transport. FXYD subunits differentially regulate the stability of the alpha subunit, maximum catalytic activity, and apparent affinity for Na^+, K^+, and ATP in a tissue specific manner (Mishra et al., 2011). FXYD1, also called phospholemman, decreases the apparent K^+ and Na^+ affinity of Na,K-ATPase (Crambert et al., 2002). However, in both adult mouse cardiac myocytes and in *Xenopus* oocyte systems, phosphorylation of FXYD1 at Ser^{68} by PKA can increase apparent Na^+ affinity and pump current (Bibert et al., 2008; Pavlovic et al., 2007). FXYD and alpha subunit proteins colocalize (Bossuyt et al., 2006; Feschenko et al., 2003; Lansbery et al., 2006), and the crystal structure of Na,K-ATPases further demonstrates that alpha and FXYD subunits physically interact (Morth et al., 2007; Shinoda et al., 2009). In rats, FXYD1 is enriched in the adult brain, specifically in the cerebellum, choroid plexus, and ependymal lining of the ventricles (Feschenko et al., 2003).

Several studies, in tissues outside the nervous system, suggest that one function of the Na,K-ATPase is to direct formation of a normal epithelium. Analysis of *Drosophila* septate junction formation suggested that regulation of these junctions by the

* Corresponding author at. Nine Cambridge Center, Rm 401, Cambridge, MA 02142, United States. fax: +1 617 258 5578.
E-mail address: sive@wi.mit.edu (H. Sive).
[1] Present address: Harvard Medical School, Department of Cell Biology, 240 Longwood Ave, Boston, MA 02115.

0012-1606/$ - see front matter © 2012 Elsevier Inc. All rights reserved.
http://dx.doi.org/10.1016/j.ydbio.2012.05.034

Na,K-ATPase occurs in a pump-independent manner (Paul et al., 2007). Conversely, tissue culture assays in MDCK cells show that levels of intracellular [Na^+] ([Na^+]$_i$), regulated by the Na,K-ATPase alpha subunit, are correlated with the amount of RhoA-GTP and epithelial junction integrity (Rajasekaran et al., 2001). The Na,K-ATPase has been implicated in regulation of tight junction proteins such as occludins and claudins, and thereby, regulation of paracellular permeability (Rajasekaran et al., 2007; Zhang et al., 2010).

In this study, we clarify the mechanisms by which the Na,K-ATPase alpha subunit, Atp1a1, regulates brain ventricle development and show for the first time a role for Fxyd1 during brain development. The data demonstrate that the Na,K-ATPase acts as a key regulator of brain ventricle formation by impacting three processes: neuroepithelium formation, neuroepithelial permeability and CSF production.

Materials and methods

Fish lines and maintenance

Danio rerio fish were raised and bred according to standard methods (Westerfield et al., 2001). Embryos were kept at 28.5 °C and staged accordingly (Kimmel et al., 1995). Lines used: wild type AB, *snakehead* (*snk ^{to273a}*) (Jiang et al., 1996), and *heart and mind* (*had^{m883}*) (Ellertsdottir et al., 2006).

Antisense morpholino oligonucleotide (MO) injection

Start site or splice-site blocking morpholino (MO) antisense oligonucleotides (Gene Tools, LLC) (Draper et al., 2001; Nasevicius and Ekker, 2000) were injected into one cell stage embryos as previously described (Graeden and Sive, 2009). The translational start site MO targets bases −11 to +14 of *atp1a1* (5′-TCTCCTC-GTCCATTTTGCTGCTTT-3′) (Yuan and Joseph, 2004) or −7 to −31 of *fxyd1* (5′-GTGGATTTAGCCTTTATCAAGCAGA-3′). Splice-site blocking MOs include, *atp1a1* (exon5–intron6), 5′-AATATAATAT-CAATAAGTACCTGGG-3′, and *fxyd1* (intron4–exon5) 5′-CTGTGA-TAATCTAGAGAGAGAGACA-3′. Concentrations used were 0.5 ng or 1 ng *atp1a1* start site MO, 2.5 ng or 7.5 ng *atp1a1* splice site MO, 7.5 ng of *fxyd1* start site MO, and 0.5 ng or 1 ng *fxyd1* splice site MO. Standard control MO used is 5′-CCTCTTACCTCAGTTACAATT-TATA-3′ and *p53* morpholino 5′-GCGCCATTGCTTTGCAAGAATTG-3′ (Gene Tools, LLC).

cDNA constructs

Full-length *atp1a1* cDNA constructs in pCS2+ were obtained from the Chen lab (Shu et al., 2003). The Quik Change II XL site directed mutagenesis kit (Stratagene) was used to modify wild type *atp1a1*, to correspond to the mutation associated with *snk ^{to273a}*, which would lead to a G to A substitution at nucleotide 812 of the coding sequence (with the resulting clone called *atp1a1GA)* (Lowery and Sive, 2005). Primers used for mutagenesis: *snkma*, 5′-CCGCACAGTCATGGATCGTATGCCACTCTCG-3′ and *snkmb*, 5′-CGAGAGTGGCAATACGATCCATGACTGTGCGG-3′. For rescue of the *atp1a1* start site morphants, the translational start site of *atp1a1-pCS2+* was mutated from 5′-AAAAGCAGCAAAAT-GGGACGAGGAGAA-3′ to 5′-AAGAGTAGTAAGATGGGTCGGGGC-GAA-3′ resulting in six mismatches within the MO target sequence thus preventing MO binding.

Full-length *fxyd1* was obtained from an EST clone (ID 6894873, Open Biosystems) and subcloned into Stu1 site in pCS2+ with a minimal Kozak consensus sequence adjacent to the initiating ATG. This cDNA clone corresponds to a clone previously identified by Sweadner and Rael (Sweadner and Rael, 2000), who suggested the provisional terminology *FXYD9dr*. However, there is no *FXYD9* in any mammalian species, and since this *FXYD* gene is most closely related to human FXYD1 (Phospholemman), we have more accurately named the zebrafish gene *fxyd1*.

C-terminal FLAG tagged Fxyd1 was generated using PCR. Briefly, primers were designed to add a linker (S–G–G–G–G–S) followed by the FLAG tag (DYKDDDDK) between the last codon and stop codon using full length *fxyd1* in pCS2+ as template. Primers used were: *fxyd1FLAGCtermF*, 5′-GTCCTTGTAGTCA-GAGCCGCCTCCACCAGAGCATTCACTCGCCCTCGCTGTGTC-3′, *fxyd1-FLAGCtermR* 5′-GACGATGACAAGTAAAAACCTGCTGACCTGAACCAA TCAGAGGAG-3′.

pCS2+RhoAV14 and *pCS2+RhoAN19* were kindly provided by R. Winklbauer (University of Toronto) and K. Symes (Boston University).

Capped *atp1a1*, *atp1a1GA*, *fxyd1*, *RhoAV14*, *RhoAN19, mGFP* and *fxyd1-FLAG* were transcribed in vitro using the SP6 mMessage mMachine kit (Ambion) after linearization. Embryos were injected at the one-cell stage with 50 pg *RhoAV14*, *fxyd1-FLAG*, or *fxyd1*, 200 pg of *atp1a1* or *atp1a1GA*, 20 pg *RhoAN19*, or 10–200 pg of *mGFP* mRNA.

RT-PCR

RNA was extracted from morphant and control embryos using Trizol reagent (Invitrogen), followed by chloroform extraction and isopropanol precipitation. RNA was pelleted by centrifugation, re-suspended in water and precipitated with $LiCl_2$. cDNA synthesis was performed using Super Script III Reverse Transcriptase (Invitrogen) plus random hexamers. PCR was then performed using primers which amplified the exonic and intronic sequence surrounding the splice MO target. Primers used include: *atp1a1 test F* 5′-CTCTTTCAAGAATTTGGTTCCC-3′, *atp1a1 test R* 5′-CTCAA-TAGAGATGGGGGTGC-3′, *fxyd1L* 5′-CACAACCACGCATCAAACTT-3′, *fxyd1R* 5′-CCGTCTCCTCTGATTGGTTC-3′. Primers used for detection of *fxyd1* reverse transcript include: *fxyd1oppL* 5′-CGGGT-CGTTTATAAGCATTGA-3′ and *fxyd1oppR* 5′-TACGGTGGATCCTCCA-CAAC-3′.

In situ hybridization

Standard methods for RNA probe synthesis containing digoxigenin (DIG)-11-UTP, hybridization and single color labeling were used as described (Sagerstrom et al., 1996). After staining, embryos were fixed in 4% paraformaldehyde overnight at 4 °C, and washed in PBT. Embryos were imaged into with a Nikon compound microscope or Zeiss dissecting scope.

Brain ventricle injections, dye retention assay, and ventricle size quantification

Brain ventricle injection and imaging have been described previously (Gutzman and Sive, 2009; Lowery and Sive, 2005).

For assaying permeability, 70 kDa MW dextran conjugated to FITC (Invitrogen; 2.5 ng/ml in water) was injected into the brain ventricles at 22 hpf and imaged at various time-points as noted in the text. Neuroepithelial permeability was quantified using ImageJ software to measure the distance of the dye front from the forebrain ventricle hinge-point. In ImageJ, the line tool was used to draw a line from the forebrain hinge-point to the dye front at a 10–20° angle from neuroepithelium. This region was chosen because it is the first and most noticeable site of dye leaking out of the wild type neuroepithelium. The net distance the dye front moved over time was calculated by subtracting the distance

at $t=0$ from other time points. Statistics were performed with GraphPad InStat software.

Forebrain ventricle area was calculated by measuring pixels per cm^2 of the forebrain ventricle with ImageJ software. Scanning confocal stacks of the full depth of the forebrain ventricle were taken and analyzed using 3D doctor (Able Software) to reconstruct the forebrain ventricle and calculate volume in μm^3.

Immunohistochemistry and western blots

Embryos were fixed in 4% PFA or 2% TCA and blocked in 2%NGS/1%Triton-X/1%BSA or 5%NGS/1%Triton-X. 50 μm transverse sections were obtained as described previously (Gutzman and Sive, 2010). Na,K-ATPase levels in whole embryos or brains (50 μg of protein) were analyzed via western blot as previously described (Gutzman and Sive, 2010). Antibodies used: Phalloidin-Texas Red/TRITC or Alexa-Fluor 633 (Molecular Probes), aPKC (Santa Cruz), Zo-1 (Invitrogen), FLAG (Sigma), propidium iodide (Invitrogen), Na,K-ATPase (alpha) (Cell Signaling Technology) and GAPDH (Abcam).

Inhibitor treatments

Dechorionated embryos were incubated in 5 mM ouabain (Sigma) diluted in embryo medium. Not all embryos responded to ouabain soaking at 16 hpf, likely due to difficulty penetrating the embryonic epidermis at this stage. 50 μM ROCK inhibitor (Calbiochem) was injected between the yolk and the brain under the midbrain and hindbrain at 14 hpf or into the brain ventricles at 22 hpf.

Intracellular Na^+ measurement

Dechorionated and deyolked embryos were collected at 24–28 hpf in 300 μl of nuclease free water. Embryos were dounce homogenized, spun at 1000 rpm, and supernatant collected. CoroNa Green (Invitrogen 10 μM) was added to the supernatant and fluorescence readings obtained using a Tecan Safire II microplate reader. A hemocytometer was used to determine number of cells per embryo (Westerfield et al., 2001).

Results

Na,K-ATPase subunits, Atp1a1 and Fxyd1, are required for brain ventricle development

In order to extend our previous findings (Lowery and Sive, 2005) and investigate the mechanisms by which the Na,K-ATPase alpha subunit, Atp1a1, regulates brain ventricle development, we tested the effect of partial loss of *atp1a1* using either a second *atp1a1* mutant allele, *had*^{m883} (*heart and mind*) (Ellertsdottir et al., 2006), or a morpholino-modified antisense oligonucleotide (MO) to inhibit zygotic pre-mRNA splicing (splice site MO)(Draper et al., 2001). In all cases, as previously described (Lowery et al., 2009; Lowery and Sive, 2005; Zhang et al., 2010), brain ventricle inflation was reduced at 24 hours post fertilization (hpf) and all images shown are representative of the phenotype observed (Fig. 1A–D; *snk*^{to273a}—65% normal ventricles ($n=39$), *had*^{m883}—70% normal ventricles ($n=55$), *atp1a1* splice—20% normal ventricles ($n=31$)). After more extensive loss of *atp1a1,* using a previously published MO (Yuan and Joseph, 2004) targeted to the translational start site (start site MO), no brain ventricle lumen was visible (Fig. 1E; 0% normal ventricles ($n=60$)) (Nasevicius and Ekker, 2000). Consistent with a dose response to Atp1a1 levels, there was a correlation between brain ventricle inflation and the amount of remaining wild type *atp1a1* RNA in *atp1a1* splice site morphants (Fig. S1C–H).

The effect of the Atp1a1 splice site MO, as identified by RT-PCR and sequencing of the resulting products, was to generate an early stop codon in the 4th extracellular loop of *atp1a1* due to the retention of intron 5 (Fig. S1A). This intron inclusion was predicted to ablate Atp1a1 pumping function. Specificity of the MO phenotypes was shown by phenotypic rescue after co-injection of the MO with 200 pg of the cognate zebrafish mRNA that does not bind the MO sequence (*atp1a1* splice rescue—100% normal ventricles ($n=31$), *atp1a1* start rescue—100% normal ventricles ($n=35$), Fig. S1B). The mRNA injected for rescue of the splice site MO had a partial, non-functional target present, while the mRNA used to rescue the start site MO was mutated to prevent MO binding.

The function of zebrafish *fxyd1* has not previously been described. *fxyd1* is expressed zygotically, that is, mRNA is not detected by RT-PCR at 3 hpf prior to mid-blastula transition (MBT), but is observed at 10 hpf after MBT when zygotic transcription begins (Fig. S1I). Consistently, we observed, by in situ hybridization, *fxyd1* expression within the embryonic brain from 10 hpf to 24 hpf (Fig. S1K–P) but not prior to MBT (data not shown). In performing controls for in situ hybridization specificity, an antisense non-protein coding transcript was reproducibly detected, and was confirmed using appropriate primers, by RT-PCR (Fig. S1I–P). This has not previously been reported for any *fxyd* gene, and the significance is unknown. However, recent data have identified a group of non-coding RNAs which may have profound regulatory function, but further investigation into a putative function of the non-coding transcript will need to be performed in the future (Ulitsky et al., 2011). Further analysis was done on the *fxyd1* protein coding transcript. Loss of function, using a splice site MO targeting the *fxyd1* protein coding strand, resulted in absence of brain ventricle inflation in 24 hpf embryos (Fig. 1F, 0% normal ventricles (n=114)), demonstrating a requirement for Fxyd1 during brain ventricle development. Specification of early brain regions in *fxyd1* morphants was normal, as judged by in situ hybridization for *pax2a*, *shh* and *krox20*, during somitogenesis (18–22 hpf). By 18 hpf, these embryos showed a shortened antero-posterior axis suggesting an earlier convergence and extension phenotype. From 24-48 hpf, *fxyd1* morphants showed severe heart edema and curved tail (data not shown). As measured by RT-PCR and sequencing of the resulting products, *fxyd1* splice site morphants have a deletion of the FXYD and transmembrane domains, due to an excision of exon 5, with no remaining wild type *fxyd1* mRNA detectable (Fig. S1A). Specificity was confirmed since the phenotype could be prevented by co-injection of 50 pg of the corresponding zebrafish mRNA that does not bind the MO (Fig. S1B; 86% normal ventricles ($n=21$)). Higher levels of *fxyd1* mRNA injected led to a lethal phenotype, indicating that the embryo is sensitive to specific levels of *fxyd1* mRNA. A second MO targeting the start site of *fxyd1,* synergized with low levels of a *fxyd1* splice site MO to give a phenotype similar to that seen with high levels of the splice site MO, further confirming specificity of morphant phenotypes (Fig. S1Q–X). The *fxyd1* splice site MO was more potent and therefore used for the rest of the study.

The severity of the *atp1a1* start site morphants, which lacked brain ventricle inflation and had abnormal neural tube refractivity, led us to examine apical polarity, marked by aPKC, and the apical junction complex using phalloidin (actin) or Zo-1 (Fig. 1G–R). In wild type embryos, junction and polarity proteins form a continuous apical band lining the ventricles (Fig. 1G, M). Partial loss of *atp1a1* does not change localization or continuity of the apical junctions (Fig. 1H–J, N–P) likely due to maternal contribution of Atp1a1. However, after greater loss of function elicited by an *atp1a1* start site MO, or by *fxyd1* splice site MO, apical junction and polarity proteins are discontinuous, with non-polarized cells crossing the midline and multiple small lumens forming (Fig. 1K–L, Q–R).

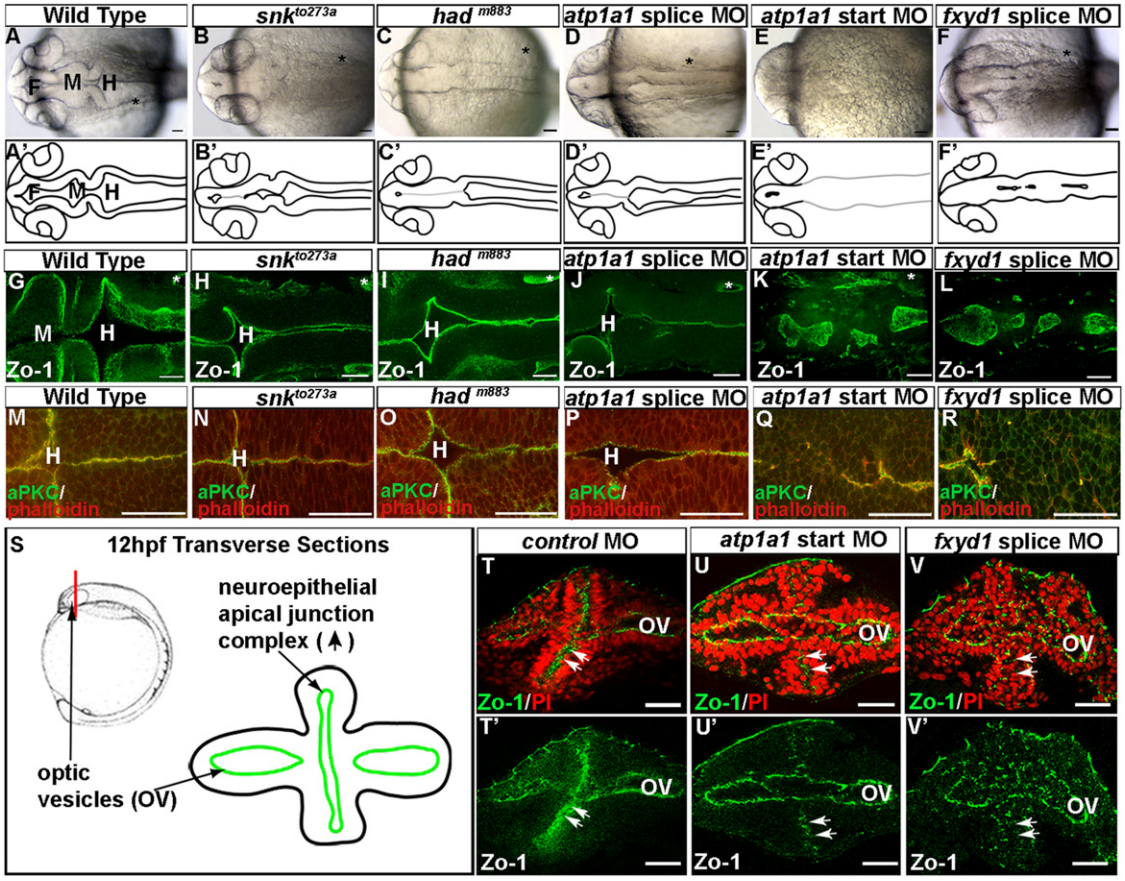

Fig. 1. The Na,K-ATPase is required for brain ventricle development. (A)–(F) Loss-of-function Na,K-ATPase embryos brightfield dorsal view images of wild type (A), partial loss of *atp1a1* with mutants *snk* ^{to273a} (B) and *had*^{m883} (C) and splice site MO (D) or severe loss of *atp1a1* with start site MO (E) and loss of *fxyd1* using a splice site MO (F). (G)–(R) Neuroepithelium formation in Na,K-ATPase morphants/mutants labeled with Zo-1 (G)–(L) or aPKC (green) and actin (phalloidin; red) (M)–(R). Images taken at 24 hpf with anterior to the left. (S) Experimental design. Red line indicates region of transverse section in 12 hpf embryo next to corresponding model of transverse section with apically localized junctions (green lines). (T)–(V) Transverse vibratome sections of 12 hpf embryos stained with Zo-1 (green) and propidium iodide (red) in control (T) *atp1a1* start site MO (U), and *fxyd1* MO (V). (T′)–(V′) Zo-1 only. Arrow indicates neuroepithelial apical junction complex. OV=optic vesicle. Asterisk=ear, F=forebrain, M=midbrain, H=hindbrain. Scale bars=50 μm.

In order to determine whether apical junctions initially form, localization of Zo-1 was examined in transverse sections of the anterior neural tube at 12 hpf, when apico-basal polarity and junctions are first established (Fig. 1S). In control embryos, Zo-1 is expressed continuously at the apical surface of the neural tube (Fig. 1T, $n=8$). Conversely, in *atp1a1* start site and *fxyd1* morphants, Zo-1 expression is patchy and scattered throughout the neuroepithelium (Fig. 1U–V; *atp1a1* start MO—$n=9$, *fxyd1* MO—$n=10$). Therefore, Atp1a1 and Fxyd1 are required during initial neuroepithelium formation.

These data show that Fxyd1 is required for formation of a correctly polarized, continuous neuroepithelium, and are the first demonstration of a function for this gene during brain development. The data also show that partial loss of *atp1a1* function leads to failure of ventricle inflation, and that more complete loss of function leads to absence of a polarized and continuous epithelium.

Atp1a1 regulates neuroepithelial permeability

Reduced brain ventricle inflation in *atp1a1* partial loss-of-function embryos may be due to either abnormal CSF production or the inability of the neuroepithelium to retain fluid. We tested whether *atp1a1* loss of function increased epithelial permeability, using a dye retention assay. In this assay, FITC-Dextran was injected into the brain ventricles at 22 hpf, and leakage of the dye out of the ventricles was monitored. A 70 kDa FITC-Dextran was chosen as it leaks out of the brain slowly, thereby allowing for identification of conditions that increase or decrease permeability. The distance traveled by the dye over time, was measured from the forebrain hinge-point to the furthest dye front, indicated by the white bar (Fig. 2A–F). This region was chosen because it is the first and most noticeable site of dye leaking out of the wild type brain (Fig. 2B). In *snk* ^{to273a} sibling embryos (wild type and heterozygotes), very little dye movement was observed (Fig. 2A–C, G). However, in *snk* ^{to273a} or *had*^{m883} mutant embryos, or after injection of *atp1a1* splice site MO, dye begins to leak out of the neuroepithelium immediately after injection (Fig. 2D–I; *snk* ^{to273a}—$n=13$, $p<.0001$; *had*^{m883}—$n=15$, $p<.001$; *atp1a1* splice MO—$n=10$, $p<.05$). Thus, although apical junction proteins properly localize, junctions do not function like wild type. Consistently, the *snk* ^{to273a} brain does not retain a 500 kDa FITC-Dextran whereas the wild type brain does demonstrating that these neuroepithelia are selectively permeable to dyes of different molecular weights (Fig. S2).

Since permeability is increased in *atp1a1* loss-of-function experiments, we hypothesized that the converse would be true, that is, that *atp1a1* overexpression in wild-type embryos would increase CSF retention relative to controls. We therefore tested neuroepithelial permeability in embryos injected with 200 pg of *atp1a1* mRNA and observed a decrease in permeability, consistent with this hypothesis (Fig. 2J, $n=10$, $p<.005$). Additionally, forebrain ventricle area and volume increased in embryos overexpressing *atp1a1*, compared to control injected embryos (Fig. S3A–B, D–E; $n=10$). We conclude that Atp1a1 regulates

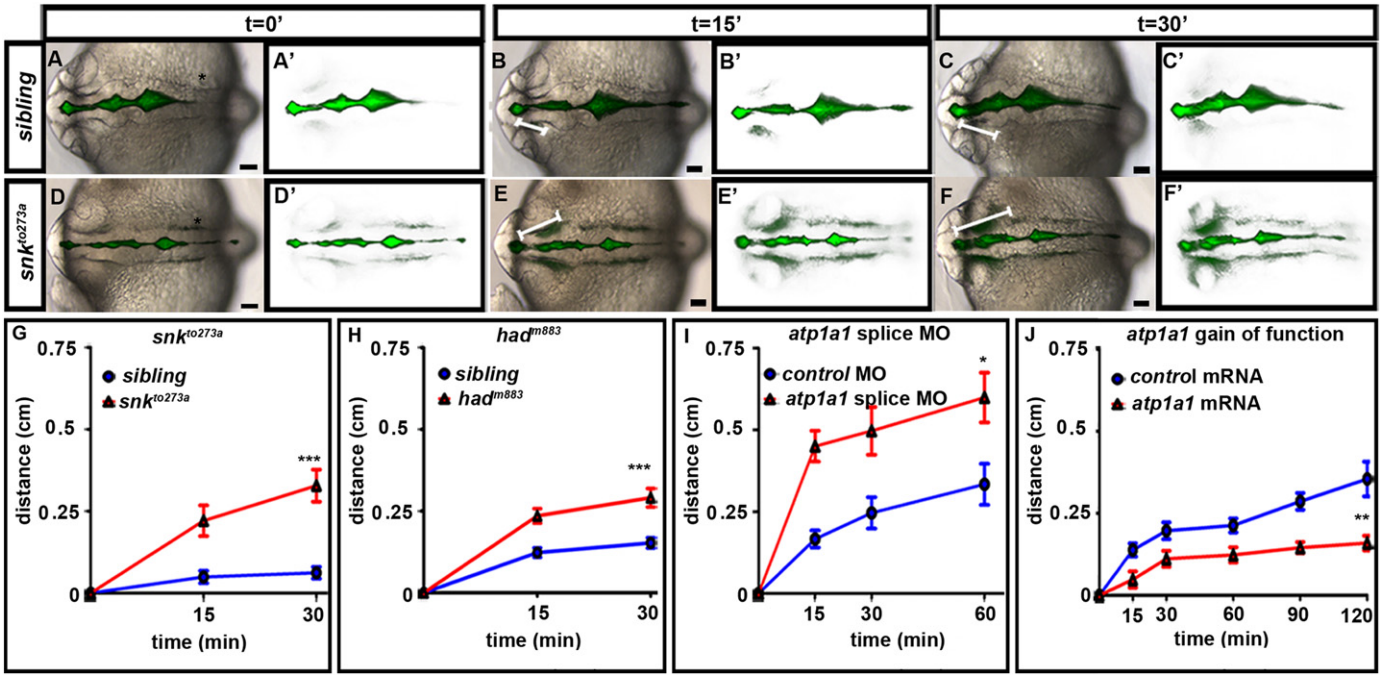

Fig. 2. Atp1a1 regulates neuroepithelial permeability. (A)–(F) Dye retention assay in sibling embryos (A)–(C) vs. *snk* ^{to273a} mutants (D)–(F). Brightfield dorsal views of embryos ventricle injected with a 70 kDa FITC Dextran (A)–(F) and corresponding dye only images (A′)–(F′) over time. The distance the dye front moves measured at each time point indicated by white line. (G)–(J) Quantification of permeability in *snk* ^{to273a} mutants (G), *had*^{m883} (H), *atp1a1* splice site morphants (I), and *atp1a1* gain-of-function embryos (J) compared to control injected. Average taken from 3–6 independent experiments and represented by mean +/− SEM. $^{***}=p<0.0001$, $^{**}=p<0.005$, $^{*}=p<0.05$ compared to control. All images taken at 22–24 hpf with anterior to left. Asterisk=ear. Scale bars=50 μm.

neuroepithelial permeability, and correlated with this, controls brain ventricle volume. Thus, part of the *snk* ^{to273a} mutant and *atp1a1* splice site morphant phenotypes is likely due to the inability of the neuroepithelium to retain CSF.

Na,K-ATPase pumping is required for brain ventricle development

The Na,K-ATPase is proposed to be a scaffolding complex as well as a pump (Krupinski and Beitel, 2009). Thus, we asked whether pumping is required for brain ventricle development. Treatment with the pump inhibitor, ouabain (Linask and Gui, 1995), at 5 hpf (mid-gastrula stage) resulted in embryos with severely disrupted apical junctions (Fig. 3A–D; 0% normal ventricles ($n=50$)), similar to the effects of injecting an *atp1a1* start site MO. Ouabain treatment at 16 hpf, after neuroepithelium formation, resulted in embryos with reduced ventricle inflation, correctly localized apical junctions (Fig. 3E–F; 25% normal ventricles ($n=67$)), but increased permeability (Fig. 3G; $n=12$, $p<.05$). Consistently, injection of mRNA encoding the putative pump-deficient *snk* ^{to273a} mutant *atp1a1* (*atp1a1GA*) (Lowery and Sive, 2005) did not rescue brain ventricle development after *atp1a1* loss of function (Fig. S4A–J) where wild type *atp1a1* mRNA rescued both neuroepithelium formation and brain ventricle inflation (Fig. S4K–L). These data show that the pump activity of zebrafish Atp1a1 is essential during brain ventricle development.

Additionally, we predicted that loss of Atp1a1 function would lead to increased intracellular Na^+ concentration ($[Na^+]_i$) in the brain, and if Fxyd1 modulates pump function, $[Na^+]_i$ would also increase in *fxyd1* loss-of-function embryos. Therefore, we measured $[Na^+]_i$ in whole embryos after inhibition of the Na,K-ATPase. Since inhibiting the Na,K-ATPase using ouabain treatment or morpholinos affects the whole body and *atp1a1* and *fxyd1* are expressed ubiquitously (Fig. S1O–P) (Canfield et al., 2002; Ellertsdottir et al., 2006), we assumed that changes in whole embryo $[Na^+]_i$ were representative of differences within the brain. Changes in $[Na^+]_i$ after Na,K-ATPase loss of funtion were quantified relative to $[Na^+]_i$ levels in control MO injected embryos, whose $[Na^+]_i$ was set equal to 1. $[Na^+]_i$ levels in control embryos was constant between several pools of embryos examined (Fig. 3H), indicating that $[Na^+]_i$ measurements can be compared between experiments. As predicted, we observed a 2.5 fold increase in $[Na^+]_i$ in embryos treated with ouabain from 5–24 hpf compared to controls (Fig. 3I, $p<.005$), and a smaller increase in those treated with ouabain from 16–24 hpf (1.3 fold; Fig. 3J). Relative to controls, $[Na^+]_i$ also increased in embryos injected with high levels of *atp1a1* start site MO (1.7 fold; $p<.05$; Fig. 3K) or *fxyd1* MO (1.5 fold; $p<.05$; Fig. 3L), and slightly after partial loss of *atp1a1* via the splice site MO (1.2 fold; Fig. 3M). We found that neuroepithelium abnormality was generally correlated with the highest $[Na^+]_i$, (Fig. 3I, K–L).

Interestingly, while both ouabain treatment from 5–24 hpf, and *atp1a1* start site MO led to similar phenotypes with regard to development of the neuroepithelium, levels of $[Na^+]_i$ in ouabain-treated embryos were higher than after injection of the *atp1a1* start site MO. This difference is likely due to inhibition of maternal Atp1a1 protein function and that of other alpha subunits by ouabain, whereas the start site MO would not inhibit maternal protein, nor affect other subunits. Consistently, levels of $[Na^+]_i$ in both *snk* ^{to273a} and *had*^{m883} mutant embryos, were higher than controls (Fig. S4M–N, *snk* $^{to273a}=2.4$ fold increase, $p<.05$; *had*$^{m883}=2.0$ fold increase, $p<.001$). The *atp1a1* missense mutant, *snk* ^{to273a} also showed somewhat higher $[Na^+]_i$ (Fig. S4M) relative to *atp1a1* start site MO (Fig. 3K) (2.4 fold for *snk* ^{to273a} versus 1.7 fold for *atp1a1* start site MO relative to controls). We hypothesized that the protein produced in *snk* ^{to273a}, retained some activity affecting $[Na^+]_i$ but not neuroepithelium formation. Consistently, injection of *atp1a1GA* mRNA into *atp1a1* start site morphants, led to elevated $[Na^+]_i$ compared to *atp1a1* start site MO alone (Fig. S4O, $p<.05$).

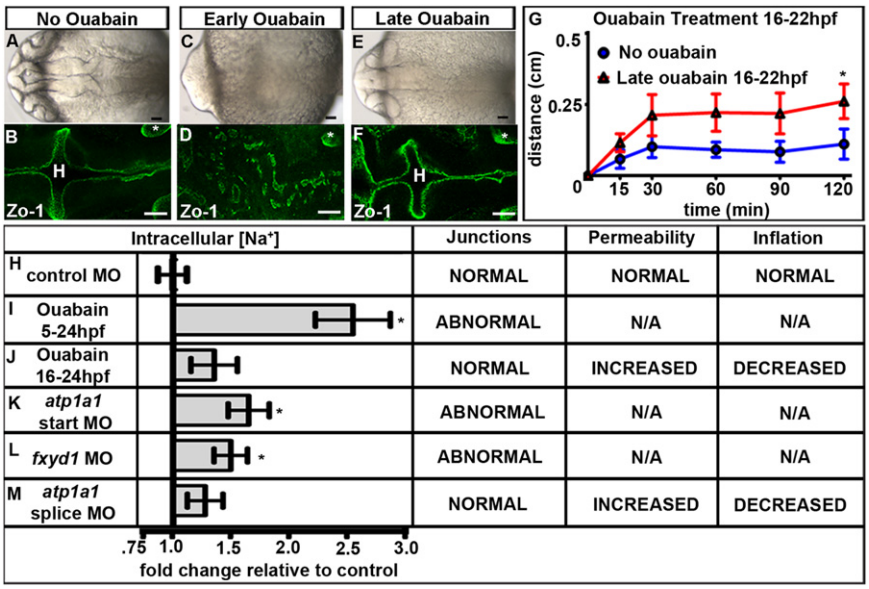

Fig. 3. Na,K-ATPase pumping is required for brain ventricle development. (A)–(F) Wild-type embryos either untreated (A)–(B) or ouabain treated from 5–24 hpf (early; C)–(D) or 16–24 hpf (late; E–F). Brightfield dorsal (A), (C), (E) or Zo-1 (B), (D), (F) images. (G) Dye retention assay in untreated (red) vs. late ouabain treated (blue) embryos. Data represented as mean +/− SEM. *$=p<.05$ compared to control. (H)–(L) Quantification of fold changes in $[Na^+]_i$ and corresponding brain ventricle phenotype. Data from 3–8 independent experiments represented as fold change compared to control MO (equal to 1) plotted as a mean +/− SEM. *$=p<0.05$ compared to control. All embryos at 24 hpf, anterior to left; Asterisk=ear, H=hindbrain. Scale bars=50 μm.

Thus, $[Na^+]_i$ increases after inhibition of Na,K-ATPase with ouabain or after knockdown of Atp1a1 or Fxyd1 subunits. Moreover, this suggests that Fxyd1 promotes Atp1a1 function, however, we cannot rule out another independent role for Fxyd1.

Atp1a1 and Fxyd1 co-regulate brain ventricle development

Data from other tissues and in vitro systems, suggest that Atp1a1 and Fxyd1 physically and functionally interact (Bibert et al., 2008; Bossuyt et al., 2006; Crambert et al., 2002; Lansbery et al., 2006; Mishra et al., 2011; Morth et al., 2007; Pavlovic et al., 2007; Shinoda et al., 2009). To determine whether Atp1a1 and Fxyd1 functionally interact, we injected embryos with low, sub-effective concentrations of *atp1a1* splice site MO and *fxyd1* MO together, which resulted in a non-cohesive neuroepithelium (0% normal ventricles ($n=17$)), whereas the individual MOs do not give a phenotype (Fig. 4A–D; *atp1a1* splice site MO=100% normal ventricles ($n=14$); *fxyd1* MO=100% normal ventricles ($n=19$)) suggesting these subunits functionally interact. Consistently, whereas embryos injected with low *atp1a1* or *fxyd1* MOs had wild type levels of $[Na^+]_i$, the combination of MOs was associated with increased $[Na^+]_i$ (Fig. 4E–G).

Studies in cell culture suggest that FXYD subunits localize, stabilize and prevent degradation of alpha subunit protein (Mishra et al., 2011). In order to ask whether similar functions for Fxyd1 were present in the developing brain, we examined Atp1a1 levels and localization in loss-of-function embryos by Western blot and immunohistochemisty. As expected, levels of Atp1a1 in *atp1a1* loss-of-function embryos were lower than controls and the protein remaining appeared as puncta enriched along the apical surface (Fig. 4H–M, O–S). In *fxyd1* morphants, levels of Atp1a1 did not decrease, in either whole embryos or dissected heads (Fig. 4H), indicating that Fxyd1 does not stabilize Atp1a1. However, Atp1a1 expression was dispersed in the *fxyd1* morphant neuroepithelium (Fig. 4N, T) demonstrating the necessity for Fxyd1 in correct localization of Atp1a1. Consistently, co-localization of Atp1a1 and Fxyd1 was observed as overlapping or adjacent protein staining of FLAG tagged Fxyd1 and endogenous Atp1a1 (Fig. 4U–V). In addition, Atp1a1 was enriched apically while Fxyd1 was present at higher levels laterally (Fig. 4W–X) suggesting some independent activity.

Consistent with discrete functions for these subunits, overexpression of 200 pg *fxyd1* mRNA in *atp1a1* start site morphants does not rescue junction formation suggesting that Fxyd1 cannot substitute for Atp1a1 function during neuroepithelium formation (Fig. 5A–H). Overexpression of *fxyd1* mRNA alone does not affect neuroepithelial permeability (Fig. 5G, M) or brain ventricle size (Fig. S3C–D). Additionally, injection of 50 pg of *fxyd1* RNA did not restore inflation or alter neuroepithelial permeability when overexpressed after partial loss of Atp1a1 function (Fig. 5G–M). The specific amounts injected were titrated to the maximum that allowed normal embryonic development. Together, these data support the conclusion that Fxyd1 does not normally regulate neuroepithelial permeability or brain ventricle inflation. Further, overexpression of *atp1a1* could not substitute for loss of Fxyd1 function in *fxyd1* morphants (Fig. 5N–S). The amount of *atp1a1* and *fxyd1* mRNA used in these assays was the same as was used to rescue the phenotypes caused by *atp1a1* or *fxyd1* MOs, respectively.

Together, the data demonstrate functional interaction, co-localization and regulation of $[Na^+]_i$ by zebrafish Fxyd1 and Atp1a1 in the developing neuroepithelium, and show that these proteins have non-redundant functions during ventricle formation.

Constitutively active RhoA rescues neuroepithelium cohesiveness but not brain ventricle inflation

Based on experiments in cell culture (Rajasekaran et al., 2001), we hypothesized that RhoA acts downstream of the Na,K-ATPase during brain ventricle development. Injection of mRNA encoding a constitutively active human RhoA, *RhoAV14,* resulted in formation of a continuous neuroepithelium in control, *atp1a1* start site, and *fxyd1* morphants (Fig. 6A–L, S5A–B; *atp1a1* start site=80% normal ventricles ($n=12$); *fxyd1* MO=80% normal ventricles ($n=20$)). However, *RhoAV14* expression in *atp1a1* start site

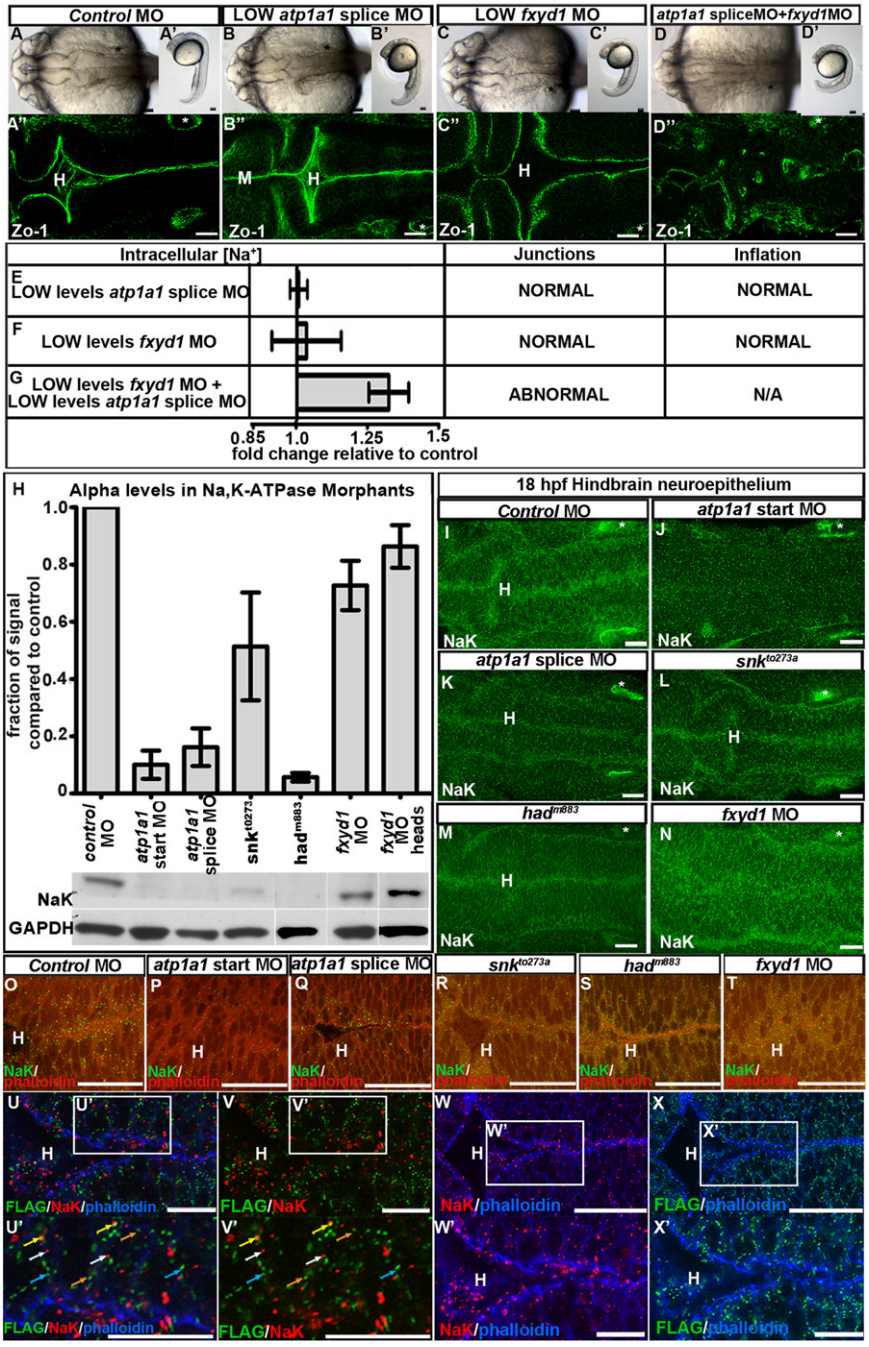

Fig. 4. Atp1a1 and Fxyd1 synergy, interaction and colocalization. (A)–(G) Atp1a1 synergizes with Fxyd1. Brightfield dorsal (A)–(D), lateral (A′)–(D′) and Zo-1 staining ((A′′)–(D′′); different embryos imaged than (A)–(D)) and measurement of $[Na^+]_i$ with corresponding brain ventricle phenotype (E)–(G), in control (A), low *atp1a1* splice MO (B,E), low *fxyd1* MO (C), (F) or together (D), (G) at 24 hpf. Data representative of 3–6 experiments as fold change relative to control=1; mean +/− SEM. (H) Western quantification of Atp1a1 (NaK) in 24 hpf whole embryos normalized to GAPDH. Representative of 3–4 independent experiments; mean +/− SEM. (I)–(T) Atp1a1 (NaK) in 18 hpf control MO (I), (O), *atp1a1* start site MO (J), (P), *atp1a1* splice site MO (K), (Q), *snk* ^{to273a} (L), (R), *had*^{m883} (M), (S) and *fxyd1* MO (N), (T). NaK alone ((I)–(N), green) or with phalloidin ((O)–(T), actin, red). (U)–(X) Localization of Atp1a1 (NaK; red) and Fxyd1-FLAG (green), phalloidin (blue) in *fxyd1* MO embryos rescued with *fxyd1-FLAG* overexpression and imaged at 24 hpf. (U′)–(X′) Higher magnification indicated by box in (U)–(X). Co-localization (yellow arrow), adjacent (orange arrow), Atp1a1 alone (white arrow) and Fxyd1 alone (blue arrow). Anterior to left. Asterisk=ear. H=hindbrain. Scale bars=10 μm (U)–(X), 50 μm (A)–(T).

morphants (Fig. 6E–H) or in *snk* ^{to273a} mutants (Fig. 6M–P) did not lead to brain ventricle inflation, suggesting that brain ventricle inflation is a RhoA independent proccess. In contrast, expression of *RhoAV14* in *fxyd1* morphants not only restored a continuous neuroepithelium, but also led to fully inflated brain ventricles (Fig. 6I–L) further supporting the hypothesis that Fxyd1 is not required for brain ventricle inflation. Expression of a dominant negative RhoA (*RhoAN19*; Fig. 6Q–R; 0% normal ventricles (n=22)) or incubation in an inhibitor of ROCK (Y27632), a target of active RhoA (Amano et al., 2000) (Fig. S5C–N), resulted in a discontinuous neuroepithelium, supporting a normal requirement for RhoA during brain development. These results suggest that Fxyd1 and Atp1a1 act through RhoA during neuroepithelium formation.

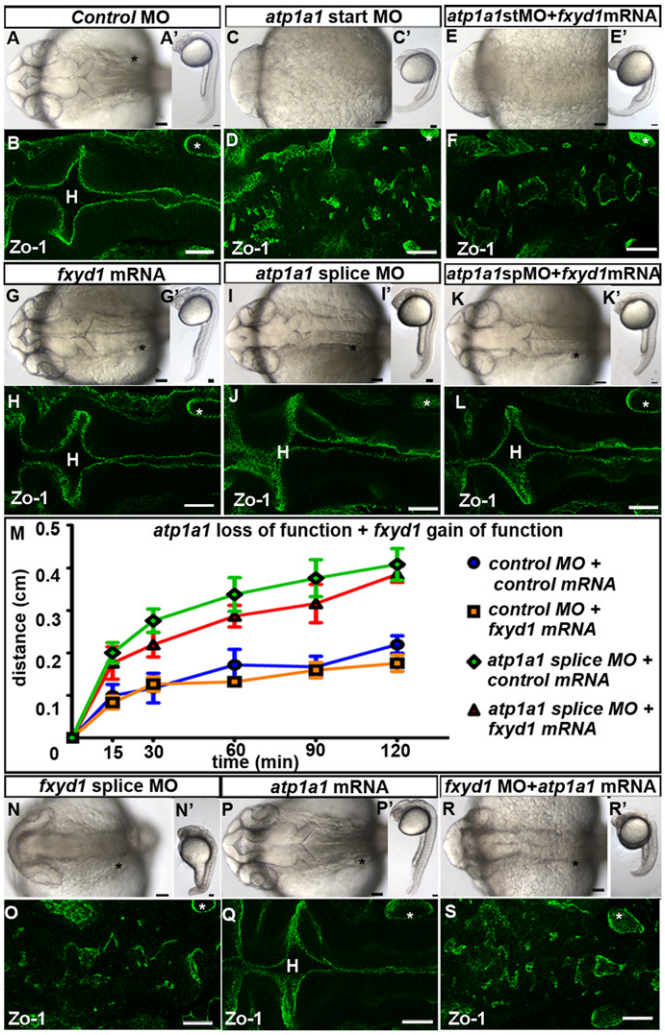

Fig. 5. Atp1a1 and Fxyd1 do not substitute for one another. (A)–(L) Overexpression of *fxyd1* in *atp1a1* loss–of–function embryos. Control (A)–(B), *atp1a1* site start MO (C)–(D), *atp1a1* start site MO+*fxyd1* mRNA (E)–(F), *fxyd1* mRNA (G)–(H), *atp1a1* splice site MO (I)–(J), and *fxyd1* mRNA+*atp1a1* splice site MO (K)–(L). (M) Neuroepithelial permeability in control MO (blue), *fxyd1* gain of function (orange), *atp1a1* splice site MO (red), and *fxyd1* mRNA+*atp1a1* splice site MO (green). Data represented as mean +/− SEM, $p > .05$. (N)–(S) *fxyd1* MO (N)–(O), *atp1a1* mRNA (P)–(Q), and *atp1a1* mRNA+ *fxyd1* MO (R)–(S). Brightfield dorsal (A)–(R) and lateral (A′)–(R′) views. Zo-1 junction staining (B), (D), (F), (H), (J), (L), (O), (Q), (S). All images taken at 24 hpf with anterior to left. Asterisk=ear. H=hindbrain. Scale bars=50 μm.

One explanation for the inability of *RhoAV14* to restore brain ventricle inflation to *snk* ^{to273a} mutants, despite a continuous neuroepithelium, is that the neuroepithelium was leaky and could not retain CSF. In wild-type embryos, expression of *RhoAV14* increased dye retention, and therefore decreased permeability (Fig. 6S; $p < .05$). Significantly, *RhoAV14* expression also decreased permeability of the *snk* ^{to273a} neuroepithelium, into the wild type range (Fig. 6T; $p < .05$), indicating that a RhoA is required for regulation of neuroepithelial permeability. Further, although *RhoA* overexpression in *snk* ^{to273a} embryos rescued neuroepithelial permeability, brain ventricle inflation remained reduced suggesting that a RhoA-insensitive process is necessary for brain ventricle inflation.

These results indicate that RhoA signaling acts downstream of Atp1a1 and Fxyd1 to regulate neuroepithelium formation and permeability. The data also delineate a RhoA-insensitive step in brain ventricle inflation, likely CSF production, which is dependent on Atp1a1, but not on Fxyd1 function.

Discussion

The Na,K-ATPase has a well-known role as a modulator of membrane potential in neurons and is essential for generating an action potential. However, this protein complex has additional activities, and this study uncovers three processes in the developing brain that are regulated by Na,K-ATPase function to culminate in the formation of the brain ventricular system: neuroepithelium polarity and junction formation, neuroepithelial permeability and CSF production (Fig. 7A). The ability of a single protein complex to regulate multiple aspects of brain ventricle formation and inflation suggests that the Na,K-ATPase is a pivotal regulator of ventricle volume.

Dissecting the activities of the Na,K-ATPase during brain ventricle formation

Several experimental approaches allowed for division of the Na,K-ATPase function into activities relevant for brain ventricle development, occurring sequentially and coordinately after neural tube closure. Formation of continuous apical neuroepithelial polarity and junctions requires RhoA activity downstream of both Atp1a1 and Fxyd1 (Fig. 7B). Na,K-ATPase pumping appears to be important in establishing rather than maintaining junctions since adding the pump inhibitor, ouabain, after initial junctions had formed, did not disrupt the neuroepithelium.

By further exploring the interface with RhoA signaling, we showed that Atp1a1 had two additional activities. RhoA could substitute for one of these functions, modulation of neuroepithelial permeability (Fig. 7C), however, the other was a RhoA-independent role uncovered by failure of RhoA to substitute for Atp1a1 during ventricle inflation, despite promoting wild type neuroepithelial permeability. This activity is likely to be CSF production (Fig. 7D). Once the neuroepithelium has formed, equilibrium between drainage from the ventricles and CSF production would maintain a normal ventricular volume. The amount of active Atp1a1 may regulate the equilibrium, since different levels of this protein can increase or decrease permeability and ventricle size. Thus, the strong phenotypes observed in Atp1a1 mutants, are likely a composite of both impaired CSF production and retention.

The role of Fxyd1 during brain ventricle development

This is the first report of a requirement for Fxyd1 function in the developing brain. *FXYD1* knockout mice show no apparent brain phenotype, suggesting functional redundancy not present in zebrafish. *FXYD1* adult null mice had increased cardiac mass, larger cardiac myocytes and, consistent with results in zebrafish, show 50% reduced Na,K-ATPase activity in mutant hearts relative to wild type (Jia et al., 2005). Fxyd1 appears to have a distinct role during brain ventricle formation, since it is required for neuroepithelium formation but, unlike Atp1a1, not for subsequent steps that lead to ventricle inflation. Consistently, overexpression of Atp1a1 does not substitute for Fxyd1, and vice versa. While synergy between *atp1a1* and *fxyd1* loss of function supports a major role for Fxyd1 as a regulator of Atp1a1 pumping, Fxyd1 may also have additional activity, that could modulate $[Na^+]_i$, for example, by inhibiting the Na^+/Ca^{2+} exchanger (Zhang et al., 2003).

Connection between Na,K-ATPase function, RhoA signaling, neuroepithelium formation and permeability

How does the Na,K-ATPase modulate RhoA function, which impacts both neuroepithelial polarity and permeability? One

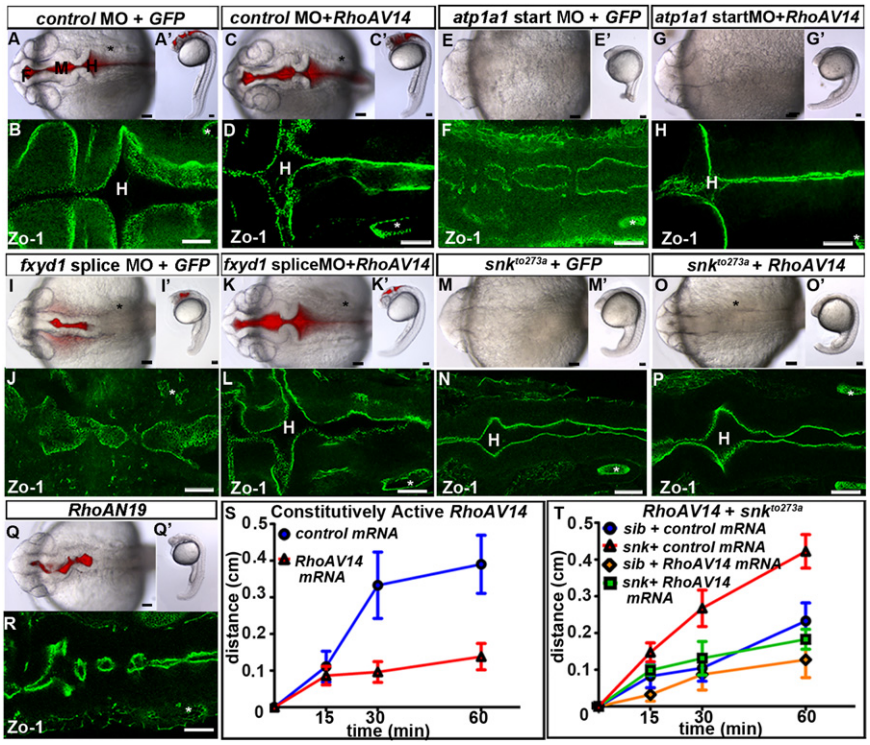

Fig. 6. Constitutively active RhoA rescues neuroepithelium formation. (A)–(H) Constitutively active *RhoAV14* (C), (D), (G), (H, (K), (L), (O), (P), or control mRNA (GFP; (A), (B), (E), (F), (I), (J), (M), (N)) in control MO (A)–(D), *atp1a1* start site MO (E)–(H), *fxyd1* MO (I)–(L), and *snk* ^{to273a} (M)–(P). (Q)–(R) Overexpression of dominant negative *RhoAN19*. (S)–(T) Dye retention assay in wild type embryos expressing control *mRNA* (blue), or *RhoAV14* (red) (S) and sibling (sib)+control *mRNA* (red), *snk* ^{to273a}+control *mRNA* (blue), sib+*RhoAV14* (orange), and *snk* ^{to273a}+*RhoAV14* (green) (T). Brightfield dorsal (A)–(Q) and lateral (A′)–(Q′) views. Ventricle injection of 2000 kDa Rhodamine Dextran dye (A), (C), (I), (K), (Q). Zo-1 (B), (D), (F), (H), (J), (L), (N), (P), (R). All images taken at 24 hpf with anterior to left. F=forebrain, M=midbrain, H=hindbrain. Asterisk=ear. Scale bars=50 μm.

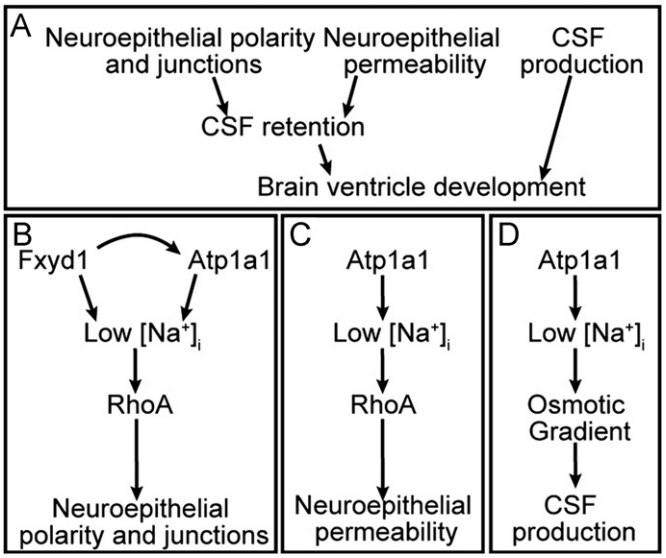

Fig. 7. Model for requirement of Na,K-ATPase during brain ventricle development. (A) Brain ventricle development is a three step process that requires establishment of neuroepithelial polarity and junctions and regulation of neuroepithelial permeability allowing for CSF retention, in addition to CSF production. Brain ventricle inflation occurs via CSF retention and CSF production. (B) Neuroepithelium formation requires RhoA which acts downstream of Fxyd1 and Atp1a1. (C) Neuroepithelial permeability requires RhoA which acts downstream of only Atp1a1. (D) CSF production is RhoA—insensitive and requires Atp1a1.

possibility is that depolarization of the cell by the Na,K-ATPase leads to RhoA activation. In cell culture, depolarization of epithelial cells activates the Ras/MEK/ERK pathway (Waheed et al., 2010), by promoting GEF activity and increasing RhoA-GTP levels. In kidney tubular cells (LLC-PK1) and MDCK cells, depolarization activates RhoA and ROCK leading to Myosin Light Chain phosphorylation (Szaszi et al., 2005). However, in no case is the mechanism connecting depolarization and RhoA activation understood.

Unlike the case in *Drosophila* trachea formation (Paul et al., 2007), our data indicate a requirement for Na,K-ATPase pump function in epithelium formation. Multiple differences between fly and vertebrate junctions (Knust and Bossinger, 2002) likely explain these different requirements for the Na,K-ATPase. Consistent with our study, Na,K-ATPase pumping is required for formation of continuous junctions and lumens in the zebrafish heart and gut (Bagnat et al., 2007; Cibrian-Uhalte et al., 2007).

We propose that RhoA regulates paracellular permeability in the zebrafish neuroepithelium, based on the size selectivity of our dye retention assay. However, we cannot rule out some contribution of vesicular transcellular pathways. Consistently, Claudin5a, a barrier claudin, and component of the tight junction complex responsible for paracellular ion transport and selectivity, is required for brain ventricle inflation and permeability (Terry et al., 2010; Zhang et al., 2010). In cell culture, RhoA activation promotes claudin phosphorylation and regulates permeability by modulating claudin–claudin interactions or recycling tight junction components (Yamamoto et al., 2008). Thus, there are plausible connections between the Na,K-ATPase, RhoA and claudins.

Modulation of CSF production by the Na,K-ATPase

Ventricle "inflation" is a scorable phenotype, but not a discrete process, as it includes formation of a non-leaky epithelium as well as CSF production, which appears to be a RhoA-insensitive

process. This is likely to be mediated by the osmotic gradient formed as a result of a membrane potential difference, under control of the Na,K-ATPase and other pumps and channels (Fig. 7D) (Brown et al., 2004; Pollay et al., 1985). Production of CSF requires both movement of water into the ventricular lumen, as well as secretion of proteins and other factors. The role of the Na,K-ATPase in water movement may occur either via Aquaporins in the plasma membrane or through the paracellular pathway. Although Aquaporin 1 is strongly expressed in the choroid plexus and knockout mice have abnormal CSF production (Oshio et al., 2003), analysis of Aquaporin activity during initial ventricle inflation has not been explored. There is little data to suggest whether Na,K-ATPase regulates protein secretion into the ventricular lumen, although one report implicates Na,K-ATPase during FGF2 secretion in primate cells (Dahl et al., 2000). Analysis of the role of Na,K-ATPase during protein secretion and water movement that results in brain ventricle inflation will be a future direction of this study.

Significance of Na,K-ATPase activity during brain ventricle volume control

Either an increase or decrease in CSF volume can be pathological throughout life (Lowery and Sive, 2009), correlating with changes in pressure and CSF composition (Desmond et al., 2005; Gato et al., 2005). Since the amount of functional Na,K-ATPase can regulate brain ventricle size in a graded manner, this pump may play a "volume sensor" and homeostatic role. The molecular basis for non-obstructive hydrocephalus is not clear, and our data suggest possible input from Na,K-ATPase function. In addition to the regulation described in this study, Na,K-ATPase activity can be fine-tuned by differential expression of beta and Fxyd subunits which modulate pump activity, expression level and correct cellular localization (Geering, 2001, 2006; Wilson et al., 2000). Therefore a slight disruption of Na,K-ATPase subunits could lead to drastic changes in activity and abnormal CSF levels.

Acknowledgments

Special thanks to Dr. Jen Gutzman, Dr. Iain Cheeseman and Sive lab members for many useful discussions and constructive criticism, and to Olivier Paugois for expert fish husbandry. This work was supported by the NIH grant MH077253 to H.L.S., an NSF fellowship to J.T.C, and an NIH NRSA fellowship to L.A.L.

Appendix A. Supporting information

Supplementary data associated with this article can be found in the online version at doi:10.1016/j.ydbio.2012.05.034.

References

Amano, M., Fukata, Y., Kaibuchi, K., 2000. Regulation and functions of Rho-associated kinase. Exp. Cell Res. 261, 44–51.
Bagnat, M., Cheung, I.D., Mostov, K.E., Stainier, D.Y., 2007. Genetic control of single lumen formation in the zebrafish gut. Nat. Cell Biol. 9, 954–960.
Bibert, S., Roy, S., Schaer, D., Horisberger, J.D., Geering, K., 2008. Phosphorylation of phospholemman (FXYD1) by protein kinases A and C modulates distinct Na,K-ATPase isozymes. J. Biol. Chem. 283, 476–486.
Bossuyt, J., Despa, S., Martin, J.L., Bers, D.M., 2006. Phospholemman phosphorylation alters its fluorescence resonance energy transfer with the Na,K-ATPase pump. J. Biol. Chem. 281, 32765–32773.
Brown, P.D., Davies, S.L., Speake, T., Millar, I.D., 2004. Molecular mechanisms of cerebrospinal fluid production. Neuroscience 129, 957–970.
Canfield, V.A., Loppin, B., Thisse, B., Thisse, C., Postlethwait, J.H., Mohideen, M.A., Rajarao, S.J., Levenson, R., 2002. Na,K-ATPase alpha and beta subunit genes exhibit unique expression patterns during zebrafish embryogenesis. Mech. Dev. 116, 51–59.
Cibrian-Uhalte, E., Langenbacher, A., Shu, X., Chen, J.N., Abdelilah-Seyfried, S., 2007. Involvement of zebrafish Na+, K+ ATPase in myocardial cell junction maintenance. J. Cell Biol. 176, 223–230.
Ciruna, B., Jenny, A., Lee, D., Mlodzik, M., Schier, A.F., 2006. Planar cell polarity signalling couples cell division and morphogenesis during neurulation. Nature 439, 220–224.
Crambert, G., Fuzesi, M., Garty, H., Karlish, S., Geering, K., 2002. Phospholemman (FXYD1) associates with Na,K-ATPase and regulates its transport properties. Proc. Nat. acad. Sci. U.S.A. 99, 11476–11481.
Dahl, J.P., Binda, A., Canfield, V.A., Levenson, R., 2000. Participation of Na,K-ATPase in FGF-2 secretion: rescue of ouabain-inhibitable FGF-2 secretion by ouabain-resistant Na,K-ATPase alpha subunits. Biochem. 39, 14877–14883.
Desmond, M.E., Levitan, M.L., Haas, A.R., 2005. Internal luminal pressure during early chick embryonic brain growth: descriptive and empirical observations. Anat. Rec. A. Discov. Mol. Cell. Evol. Biol. 285, 737–747.
Draper, B.W., Morcos, P.A., Kimmel, C.B., 2001. Inhibition of zebrafish fgf8 pre-mRNA splicing with morpholino oligos: a quantifiable method for gene knockdown. Genesis 30, 154–156.
Ellertsdottir, E., Ganz, J., Durr, K., Loges, N., Biemar, F., Seifert, F., Ettl, A.K., Kramer-Zucker, A.K., Nitschke, R., Driever, W., 2006. A mutation in the zebrafish Na,K-ATPase subunit atp1a1a.1 provides genetic evidence that the sodium potassium pump contributes to left-right asymmetry downstream or in parallel to nodal flow. Dev. Dyn. 235, 1794–1808.
Feschenko, M.S., Donnet, C., Wetzel, R.K., Asinovski, N.K., Jones, L.R., Sweadner, K.J., 2003. Phospholemman, a single-span membrane protein, is an accessory protein of Na,K-ATPase in cerebellum and choroid plexus. J. Neurosci. 23, 2161–2169.
Gato, A., Moro, J.A., Alonso, M.I., Bueno, D., De La Mano, A., Martin, C., 2005. Embryonic cerebrospinal fluid regulates neuroepithelial survival, proliferation, and neurogenesis in chick embryos. Anat. Rec. A. Discov. Mol. Cell. Evol. Biol. 284, 475–484.
Geering, K., 2001. The functional role of beta subunits in oligomeric P-type ATPases. J. Bioenerg. Biomembr. 33, 425–438.
Geering, K., 2006. FXYD proteins: new regulators of Na-K-ATPase. American J. Physiol. Renal Physiol. 290, F241–F250.
Graeden, E., Sive, H., 2009. Live imaging of the zebrafish embryonic brain by confocal microscopy. J. Visualized Exp. (26), e1217. 〈http://dx.doi.org/10.3791/1217〉.
Gutzman, J.H., Sive, H., 2009. Zebrafish brain ventricle injection. J. Visualized Exp. (26), e1218. 〈http://dx.doi.org/10.3791/1218〉.
Gutzman, J.H., Sive, H., 2010. Epithelial relaxation mediated by the myosin phosphatase regulator Mypt1 is required for brain ventricle lumen expansion and hindbrain morphogenesis. Development 137, 795–804.
Hong, E., Brewster, R., 2006. *N*-cadherin is required for the polarized cell behaviors that drive neurulation in the zebrafish. Development 133, 3895–3905.
Jia, L.G., Donnet, C., Bogaev, R.C., Blatt, R.J., McKinney, C.E., Day, K.H., Berr, S.S., Jones, L.R., Moorman, J.R., Sweadner, K.J., Tucker, A.L., 2005. Hypertrophy, increased ejection fraction, and reduced Na-K-ATPase activity in phospholemman-deficient mice. Am. J. Physiol.—Heart Circ. Physiol. 288, H1982–H1988.
Jiang, Y.J., Brand, M., Heisenberg, C.P., Beuchle, D., Furutani-Seiki, M., Kelsh, R.N., Warga, R.M., Granato, M., Haffter, P., Hammerschmidt, M., Kane, D.A., Mullins, M.C., Odenthal, J., van Eeden, F.J., Nusslein-Volhard, C., 1996. Mutations affecting neurogenesis and brain morphology in the zebrafish, Danio rerio. Development 123, 205–216.
Kimmel, C.B., Ballard, W.W., Kimmel, S.R., Ullmann, B., Schilling, T.F., 1995. Stages of embryonic development of the zebrafish. Dev. Dyn. 203, 253–310.
Knust, E., Bossinger, O., 2002. Composition and formation of intercellular junctions in epithelial cells. Science 298, 1955–1959.
Krupinski, T., Beitel, G.J., 2009. Unexpected roles of the Na,K-ATPase and other ion transporters in cell junctions and tubulogenesis. Physiology (Bethesda) 24, 192–201.
Lansbery, K.L., Burcea, L.C., Mendenhall, M.L., Mercer, R.W., 2006. Cytoplasmic targeting signals mediate delivery of phospholemman to the plasma membrane. Am. J. Physiol.—Cell Physiol. 290, C1275–C1286.
Linask, K.K., Gui, Y.H., 1995. Inhibitory effects of ouabain on early heart development and cardiomyogenesis in the chick embryo. Dev. Dyn. 203, 93–105.
Lowery, L.A., De Rienzo, G., Gutzman, J.H., Sive, H., 2009. Characterization and classification of zebrafish brain morphology mutants. Anat. Rec. (Hoboken) 292, 94–106.
Lowery, L.A., Sive, H., 2005. Initial formation of zebrafish brain ventricles occurs independently of circulation and requires the nagie oko and snakehead/atp1a1a.1 gene products. Development 132, 2057–2067.
Lowery, L.A., Sive, H., 2009. Totally tubular: the mystery behind function and origin of the brain ventricular system. Bioessays 31, 446–458.
Mishra, N.K., Peleg, Y., Cirri, E., Belogus, T., Lifshitz, Y., Voelker, D.R., Apell, H.J., Garty, H., Karlish, S.J., 2011. FXYD proteins stabilize Na,K-ATPase: amplification of specific phosphatidylserine-protein interactions. J. Biol. Chem. 286, 9699–9712.
Morth, J.P., Pedersen, B.P., Toustrup-Jensen, M.S., Sorensen, T.L., Petersen, J., Andersen, J.P., Vilsen, B., Nissen, P., 2007. Crystal structure of the sodium–potassium pump. Nature 450, 1043–1049.
Nasevicius, A., Ekker, S.C., 2000. Effective targeted gene 'knockdown' in zebrafish. Nat. Genet. 26, 216–220.

Oshio, K., Song, Y., Verkman, A.S., Manley, G.T., 2003. Aquaporin-1 deletion reduces osmotic water permeability and cerebrospinal fluid production. Acta. Neurochir. Suppl. 86, 525–528.
Paul, S.M., Palladino, M.J., Beitel, G.J., 2007. A pump-independent function of the Na,K-ATPase is required for epithelial junction function and tracheal tube-size control. Development 134, 147–155.
Pavlovic, D., Fuller, W., Shattock, M.J., 2007. The intracellular region of FXYD1 is sufficient to regulate cardiac Na,K-ATPase. FASEB J. 21, 1539–1546.
Pollay, M., Hisey, B., Reynolds, E., Tomkins, P., Stevens, F.A., Smith, R., 1985. Choroid plexus Na+/K+-activated adenosine triphosphatase and cerebrospinal fluid formation. Neurosurgery 17, 768–772.
Rajasekaran, S.A., Barwe, S.P., Gopal, J., Ryazantsev, S., Schneeberger, E.E., Rajasekaran, A.K., 2007. Na,K-ATPase regulates tight junction permeability through occludin phosphorylation in pancreatic epithelial cells. Am. Physiol. Soc.—Gastrointest. Liver Physiol. 292, G124–G133.
Rajasekaran, S.A., Palmer, L.G., Moon, S.Y., Peralta Soler, A., Apodaca, G.L., Harper, J.F., Zheng, Y., Rajasekaran, A.K., 2001. Na,K-ATPase activity is required for formation of tight junctions, desmosomes, and induction of polarity in epithelial cells. Mol. Biol. Cell 12, 3717–3732.
Sagerstrom, C.G., Grinbalt, Y., Sive, H., 1996. Anteroposterior patterning in the zebrafish, Danio rerio: an explant assay reveals inductive and suppressive cell interactions. Development 122, 1873–1883.
Shinoda, T., Ogawa, H., Cornelius, F., Toyoshima, C., 2009. Crystal structure of the sodium–potassium pump at 2.4 A resolution. Nat. 459, 446–450.
Shu, X., Cheng, K., Patel, N., Chen, F., Joseph, E., Tsai, H.J., Chen, J.N., 2003. Na,K-ATPase is essential for embryonic heart development in the zebrafish. Development 130, 6165–6173.
Speake, T., Whitwell, C., Kajita, H., Majid, A., Brown, P.D., 2001. Mechanisms of CSF secretion by the choroid plexus. Microsc. Res. Tech. 52, 49–59.
Sweadner, K.J., Rael, E., 2000. The FXYD gene family of small ion transport regulators or channels: cDNA sequence, protein signature sequence, and expression. Genomics 68, 41–56.
Szaszi, K., Sirokmany, G., Di Ciano-Oliveira, C., Rotstein, O.D., Kapus, A., 2005. Depolarization induces Rho–Rho kinase-mediated myosin light chain phosphorylation in kidney tubular cells. Am. J. Physiol.—Cell Physiol. 289, C673–C685.
Terry, S., Nie, M., Matter, K., Balda, M.S., 2010. Rho signaling and tight junction functions. Physiology (Bethesda) 25, 16–26.
Ulitsky, I., Shkumatava, A., Jan, C.H., Sive, H., Bartel, D.P., 2011. Conserved function of lincRNAs in vertebrate embryonic development despite rapid sequence evolution. Cell 147, 1537–1550.
Waheed, F., Speight, P., Kawai, G., Dan, Q., Kapus, A., Szaszi, K., 2010. Extracellular signal-regulated kinase and GEF-H1 mediate depolarization-induced Rho activation and paracellular permeability increase. Am. J. Physiol.—Cell Physiol. 298, C1376–C1387.
Welss, P., 1934. Secretory activity of the inner layer of the embryonic mid-brain of the chick, as revealed by tissue culture. The Anatomical Record 58, 299–302.
Westerfield, M., Sprague, J., Doerry, E., Douglas, S., Grp, Z., 2001. The Zebrafish Information Network (ZFIN): a resource for genetic, genomic and developmental research. Nucleic Acids Res. 29, 87–90.
Wilson, P.D., Devuyst, O., Li, X., Gatti, L., Falkenstein, D., Robinson, S., Fambrough, D., Burrow, C.R, 2000. Apical plasma membrane mispolarization of NaK-ATPase in polycystic kidney disease epithelia is associated with aberrant expression of the beta2 isoform. Am. J. Pathol. 156, 253–268.
Yamamoto, M., Ramirez, S.H., Sato, S., Kiyota, T., Cerny, R.L., Kaibuchi, K., Persidsky, Y., Ikezu, T., 2008. Phosphorylation of claudin-5 and occludin by rho kinase in brain endothelial cells. Am. J. Pathol. 172, 521–533.
Yuan, S., Joseph, E.M., 2004. The small heart mutation reveals novel roles of Na+/K+-ATPase in maintaining ventricular cardiomyocyte morphology and viability in zebrafish. Circ. Res. 95, 595–603.
Zhang, J., Piontek, J., Wolburg, H., Piehl, C., Liss, M., Otten, C., Christ, A., Willnow, T.E., Blasig, I.E., Abdelilah-Seyfried, S., 2010. Establishment of a neuroepithelial barrier by Claudin5a is essential for zebrafish brain ventricular lumen expansion. Proc. Nat. acad. Sci. U.S.A. 107, 1425–1430.
Zhang, X.Q., Qureshi, A., Song, J., Carl, L.L., Tian, Q., Stahl, R.C., Carey, D.J., Rothblum, L.I., Cheung, J.Y., 2003. Phospholemman modulates Na+/Ca2+ exchange in adult rat cardiac myocytes. Am. J. Physiol.—Heart Circ. Physiol. 284, H225–H233.